

Supporting Information

Heating and Cooling of Ligand-Coated Colloidal Nanocrystals in Solid Films and Solvent Matrices

Benjamin T. Diroll^{1*} and Richard D. Schaller^{1,2}

¹Center for Nanoscale Materials, Argonne National Laboratory, Lemont, IL 60439

²Department of Chemistry, Northwestern University, Evanston, IL 60208

[*bdiorl@anl.gov](mailto:bdiorl@anl.gov)

Supporting Methods and Data

Materials

Cadmium nitrate tetrahydrate (98 %), sodium myristate (>99 %), cadmium acetate (98 %), selenium powder (99.99 %), octadecene (90 %), oleic acid (90 %), carbon disulfide (99.9 %), carbon tetrachloride (99.9 %), tetrachloroethylene (> 99 %), chloroform-d (99.96 % D-atom), heptane-d₁₆ (99 % D atom), hexane-d14 (99 % D atom), cyclohexane-d₁₂ (99.6 % D atom), methylcyclohexane-d₁₄ (99.5 % D atom), toluene-d₈ (99.6 %) were purchased from Sigma-Aldrich. Other solvents used were ACS grade or higher.

Methods

Synthesis. 4 monolayer CdSe nanoplatelets were synthesized following standard literature recipes.^{35,36} 170 mg of cadmium myristate, 15 mL octadecene, and 12 mg of Se powder were added to a 50 mL three neck flask and degassed under vacuum at room temperature for 30 minutes, then heated under nitrogen to 240 °C. At 195 °C, 40 mg of finely-ground cadmium acetate powder was added under nitrogen counterflow. After 5 minutes the reaction was stopped by removing the heating mantle. While cooling, 2 mL of oleic acid was injected at 120 °C and 10 mL of hexanes was added to dilute the reaction. The nanoplatelets were isolated by centrifugation at 15000 rpm for 10 minutes and redispersed into hexanes. Subsequently the nanoplatelets were washed two more times by ethanol precipitation to remove excess unbound oleic acid ligands. These washed particles were stored in hexanes, which was used as the mother stock for all measured solutions and thin films. A solid film was prepared by drop-casting the concentrated hexane stock; solutions in studied solvent matrices were prepared by first evaporating the hexanes dispersion to dryness under gentle nitrogen flow, then redispersing with sonication in 300 µL of the desired solvent.

Spectroscopy. UV-visible spectra were collected using a Cary 50 or Cary 60 instrument equipped with temperature-control stage for cuvettes. Except for those static temperature measurements explicitly above 295 K, all measurements were performed at 295 K. IR absorption spectra were collected using a Nicolet 6700 FT-IR. Infrared pump, electronic probe (IPEP) measurements were performed using the output, at 3460 nm, of an optical parametric amplifier driven by an 800 nm 30 fs Ti: sapphire laser running at 2 kHz. To enhance the available power, this beam path was placed under nitrogen purge. The probe light was delayed using a mechanical delay stage, with supercontinuum white light generated using the 800 nm beam focused into a sapphire crystal. Transient absorption spectra were collected using a mechanical chopper to block half of the pump pulses. Excepting the solid film, measurements were performed using 1 mm quartz cuvettes with high optical transparency both as the pump and the probe wavelengths. For samples which were relatively poorly dispersed in solution, stirring was performed to prevent settling. The temperature of the nanoplatelets in IPEP experiments (generating $\Delta\alpha$) was estimated from static absorption measurements (generating ΔA) by comparison of the integrated intensity of the heavy-hole induced absorption feature in both types of measurement. Dynamics

were probed at the induced absorption feature of the heavy hole (reddest feature of IPEP measurements). This provides the best spectral isolation and strongest signal.

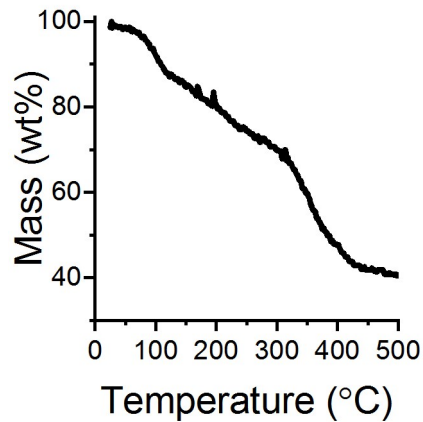


Figure S1. Thermogravimetric analysis of washed 4 ML CdSe nanoplatelet sample. Temperature was ramped in an air atmosphere at 20 °C/minute to 500 °C. Assuming the entire weight loss is due to loss of oleate ligands, the organic weight fraction was 59 %. For the dimensions of the CdSe nanoplatelet sample used in this work, assuming bulk zinc blende CdSe density, this corresponds to 1.8 ligands/nm².

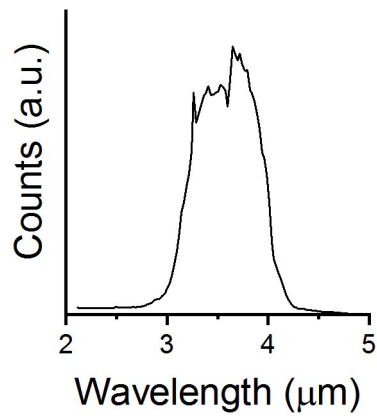


Figure S2. Spectrum of the pump beam for an optical parametric amplifier output at 3460 nm.

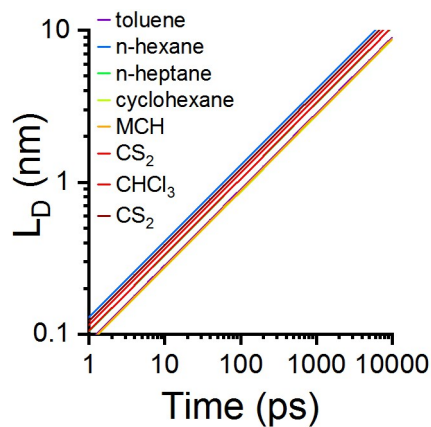


Figure S3. Characteristic self-diffusion length of n-hexane versus time. The diffusion length is calculated from $(4Dt)^{1/2}$, where the diffusivity D was based upon literature reports.¹⁻⁶

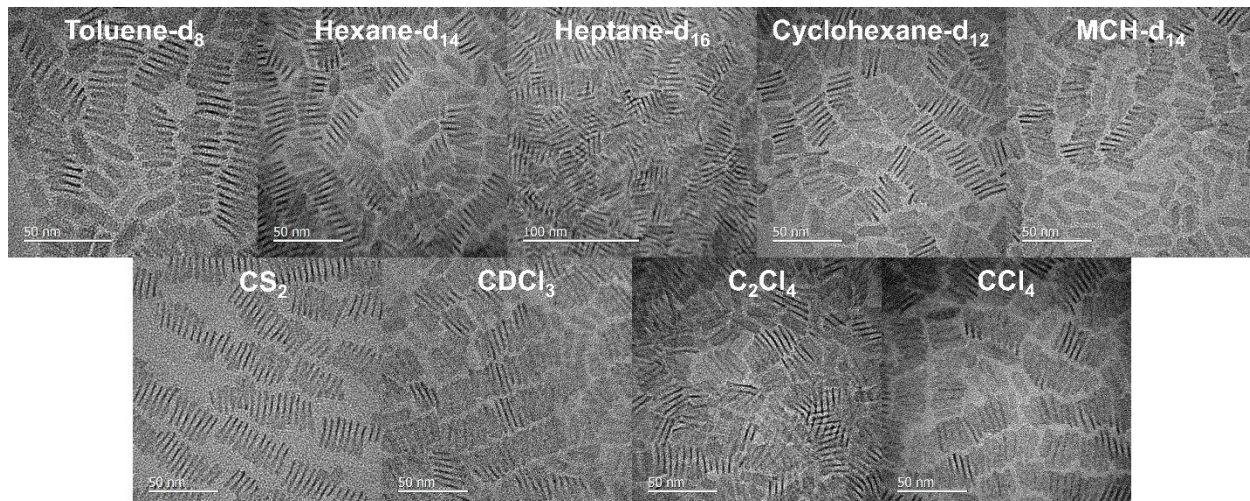


Figure S4. Transmission electron microscope micrographs of the same 4 ML nanoplatelet sample cast from the specified solvents on to carbon coated copper TEM grids. The samples showed some differences in aggregation state, but did not show any gross morphological changes. The aggregation in the dried solids is also not necessarily reflective of the solution state, which is analyzed in Table S1.

Table S1. Table of extinction values at the band edge excitonic absorption (512 nm) and 550 nm for the measured samples.

Solvent	Extinction at 512 nm (OD)	Extinction at 550 nm (OD)	OD ₅₁₂ /OD ₅₅₀ [*]
toluene-d ₈	0.547	0.069	0.12614
hexane-d ₁₄	0.705	0.027	0.0383
heptane-d ₁₆	0.5798	0.089	0.1535
cyclohexane-d ₁₂	1.1	0.008	0.00727
methylcyclohexane-d ₁₄	0.7	0.003	0.00429
CS ₂	0.356	0.007	0.01966
CDCl ₃	0.472	0.0188	0.03983
C ₂ Cl ₄	0.492	0.109	0.22154

CCl ₄	0.522	0.02	0.03831
solid film	0.112	0.009	0.08036

*A higher ratio is indicative of more scattering.

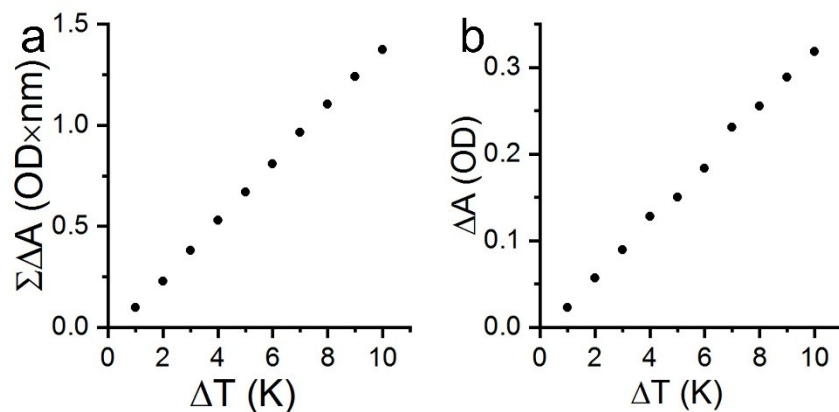


Figure S5. Temperature calibration obtained from static absorption measurements referenced to the absorption of the sample at 295 K. In (a) The data points represent an integration (via the trapezoid approximation) of the heavy hole induced absorption feature in static absorption measurements (see Figure 1c). Increments of wavelength are used to the x-axis and increments of ΔA for used for the y-axis of the sum. (The same units can be used in transient spectra.) This calibration curve was used to determine temperature changes in from IPEP spectra. (b) Raw static change in absorbance from static absorption measurements referenced to 295 K, for 516 nm, the peak in the difference curves. Although this also yields a linear change over the measured temperature range, the higher resolution of the static absorption measurements (compared to transient absorption) would lead to systematic underestimation of the temperature changes of IPEP spectra.

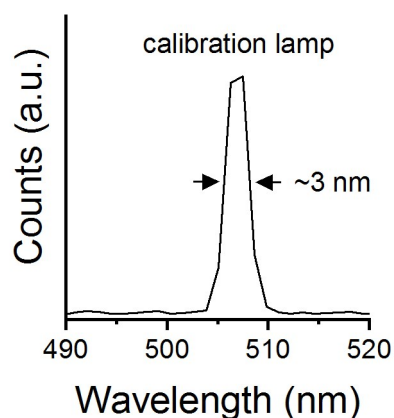


Figure S6. Spectral resolution test of transient absorption spectrometer close to the wavelength of experiments. The band-width of a lamp line in the test was approximately 3 nm. The line-width of the lamp feature was 0.3 nm and therefore the 3 nm line-width reflects the spectrometer resolution limit.

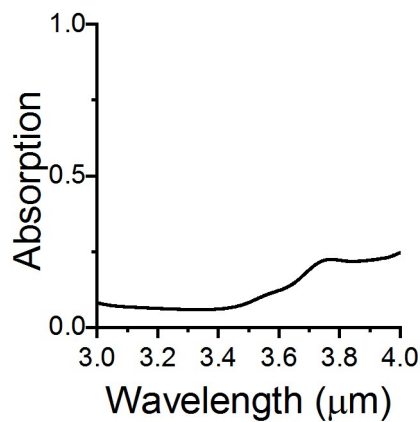


Figure S7. Absorption from 1 mm pathlength quartz cuvette used for IPEP experiments.

References

- (1) Jonas, J.; Hasha, D.; Huang, S. G. Self-Diffusion and Viscosity of Methylcyclohexane in the Dense Liquid Region. *J. Chem. Phys.* **1979**, *71* (10), 3996–4000.
- (2) Harris, K. R. Temperature and Density Dependence of the Self-Diffusion Coefficient of n-Hexane from 223 to 333 K and up to 400 MPa. *J. Chem. Soc. Faraday Trans. 1 Phys. Chem. Condens. Phases* **1982**, *78* (7), 2265–2274.
- (3) Watts, H.; Alder, B. J.; Hildebrand, J. H. Self-Diffusion of Carbon Tetrachloride, Isobars and Isochores. *J. Chem. Phys.* **1955**, *23* (4), 659–661.
- (4) Golubev, V. A.; Gurina, D. L.; Kumeev, R. S. Self-Diffusion and Heteroassociation in an Acetone–Chloroform Mixture at 298 K. *Russ. J. Phys. Chem. A* **2018**, *92* (1), 75–78.
- (5) O'Reilly, D. E.; Peterson, E. M. Self-Diffusion Coefficients and Rotational Correlation Times in Polar Liquids. III. Toluene. *J. Chem. Phys.* **1972**, *56* (5), 2262–2266.
- (6) Albright, J. G.; Aoyagi, K. The Mutual Diffusion Study in the Systems Containing Benzene or Benzene- d 6 at 25 ° . *J. Chem. Phys.* **2003**, *64* (1), 81–83.